



# A Small Molecule Inhibits Protein Disulfide Isomerase and Triggers the Chemosensitization of Cancer Cells\*\*

Jürgen Eirich, Simone Braig, Liliana Schyschka, Phil Servatius, Judith Hoffmann, Sabrina Hecht, Simone Fulda, Stefan Zahler, Iris Antes, Uli Kazmaier, Stephan A. Sieber,\* and Angelika M. Vollmar\*

**Abstract:** Resistance to chemotherapeutic agents represents a major challenge in cancer research. One approach to this problem is combination therapy, the application of a toxic chemotherapeutic drug together with a sensitizing compound that addresses the vulnerability of cancer cells to induce apoptosis. Here we report the discovery of a new compound class (**T8**) that sensitizes various cancer cells towards etoposide treatment at subtoxic concentrations. Proteomic analysis revealed protein disulfide isomerase (PDI) as the target of the **T8** class. In-depth chemical and biological studies such as the synthesis of optimized compounds, molecular docking analyses, cellular imaging, and apoptosis assays confirmed the unique mode of action through reversible PDI inhibition.

The resistance of tumor cells to drugs results from numerous genetic and epigenetic changes.<sup>[1]</sup> Cancer cells by nature require increased protein synthesis and thus respond to endoplasmic reticulum (ER) stress by activating the unfolded protein response (UPR) which is mediated by ER chaperones such as protein disulfide isomerase (PDI).<sup>[1c,2]</sup>

As ER chaperones maintain ER homeostasis and support cancer cell survival, interest has emerged in targeting these proteins to fight chemoresistance. In this respect PDI has received increasing attention and the crystal structures of the human full-length protein have recently been published.<sup>[3]</sup> The isomerase is organized in four distinct domains (a, a' and b, b'). The a and a' domains are catalytically active and share

significant homology. PDI catalyzes thiol–disulfide exchange reactions of both intra- and intermolecular disulfides.<sup>[4]</sup> The role of this enzyme in diseases reaches far beyond cancer and was recently reviewed in detail.<sup>[5]</sup> Although several inhibitors were published in recent years<sup>[6–12]</sup> the most specific compounds—16F16, RB-11-ca, PACMA 31, and P1—exhibit a pharmacologically less desired irreversible mode of action. Here we introduce reversible and highly specific PDI inhibitors that sensitize tumor cells towards classical chemotherapeutic agents.

The screening of a commercial compound library for the chemosensitization of etoposide-induced apoptosis in various cancer cell lines revealed **T8** as a promising candidate. The combination of subtoxic concentrations of etoposide (500 nM) and **T8** dose-dependently led to pronounced apoptosis rates with a minimal concentration of 25  $\mu$ M **T8** in a leukemic (Jurkat) as well as in a breast cancer cell line (MDA-MB-231) (Figure 1 A). In addition, the long-term survival of Jurkat cells was synergistically inhibited after treatment with a combination of etoposide and **T8** (Figure 1 B). Growth of various carcinoma cell lines such as LNCAP (prostate cancer), PancTu1, and L3.6pl (pancreas cancer) was also strongly affected by the combined treatment with other chemotherapeutic drugs such as doxorubicin or TRAIL and **T8** (Figures S1 and S2). In contrast, noncancerous human endothelial cells (HUVEC) did not respond to **T8** in combination with etoposide or doxorubicin (Figure S3).

[\*] Dr. J. Eirich,<sup>[§]</sup> Prof. Dr. I. Antes, Prof. Dr. S. A. Sieber  
Center for Integrated Protein Science Munich CIPSM  
Department of Chemistry, Institute of Advanced Studies IAS  
Technische Universität München  
Lichtenbergstrasse 4, 85747 Garching (Germany)  
E-mail: stephan.sieber@tum.de

Dr. S. Braig,<sup>[†]</sup> Dr. L. Schyschka, Prof. Dr. S. Zahler,  
Prof. Dr. A. M. Vollmar  
Department of Pharmacy, Center for Drug Research  
Pharmaceutical Biology, Ludwig-Maximilians-Universität München  
Butenandtstrasse 5–13, 81377 München (Germany)  
E-mail: angelika.vollmar@cup.uni-muenchen.de  
P. Servatius, J. Hoffmann, Prof. Dr. U. Kazmaier  
Institute for Organic Chemistry, Saarland University  
Im Stadtwald, Geb. C4.2, 66123 Saarbrücken (Germany)  
Prof. Dr. S. Fulda  
Institute for Experimental Cancer Research in Pediatrics  
University Hospital Frankfurt  
Kometurstrasse 3a, 60528 Frankfurt a. M. (Germany)

S. Hecht, Prof. Dr. I. Antes  
Department of Life Sciences, Technische Universität München  
Emil-Erlenmeyer-Forum 8, 85354 Freising-Weihenstephan  
(Germany)

[§] Current address: Department of Oncology/Pathology  
Cancer Proteomics Mass Spectrometry  
SciLifeLab Stockholm, Karolinska Institutet  
Tomtebodavägen 23, 17165 Solna (Sweden)

[†] These authors contributed equally to this work.

[\*\*] We thank Mona Wolff, Katja Bäuml, and Burghard Cordes for excellent scientific support, Dr. Stuppner and Dr. Langner (University of Innsbruck) for collaboration. S.A.S. was supported by the Deutsche Forschungsgemeinschaft (SFB749, SFB1035, and FOR1406), an ERC starting grant, and the Center for Integrated Protein Science Munich CIPSM, J.E. thanks the TUM Graduate School and A.M.V. thanks the DFG and the Wilhelm Sander Foundation.



Supporting information for this article (synthesis and characterization of compounds, bioassays, cell biology as well as proteome preparation, labeling, and mass spectrometry) is available on the WWW under <http://dx.doi.org/10.1002/anie.201406577>.

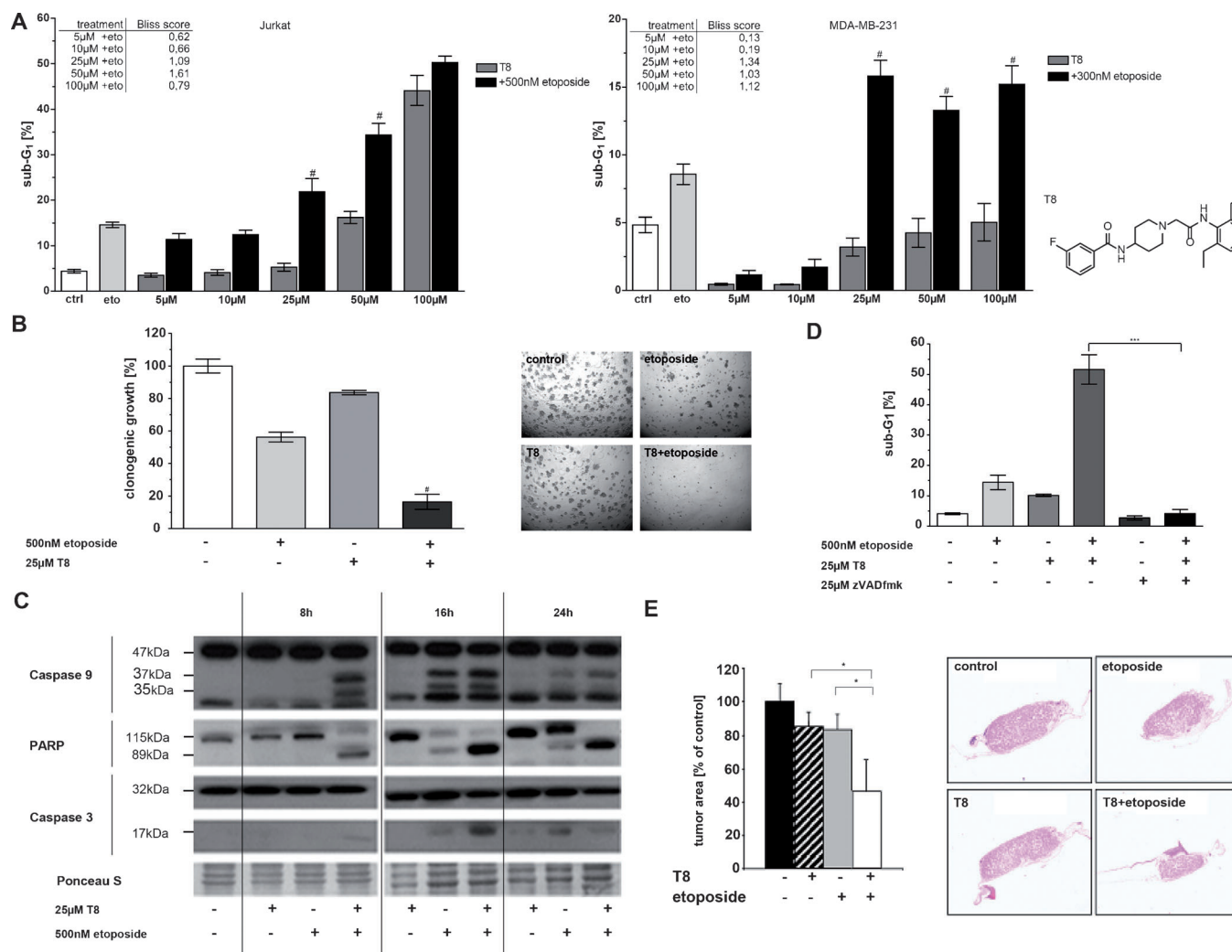


**Figure 1.** T8 sensitizes cancer cell lines towards etoposide-induced cell death. A) Apoptosis assay by FACS analysis; chemical structure of T8. B) Long-term growth analysis of Jurkat cells after treatment. C) Activation of caspases (western blot analysis). D) Effect of caspase inhibition by zVADfmk. E) Effect on CAM-based tumor growth (L3.6pl pancreatic carcinoma cells). \*\*\* $p < 0.001$ ; \* $p < 0.05$ ; # synergistic.

Corresponding western blot analysis illustrated increased hallmarks of apoptosis such as PARP cleavage and caspase-9 as well as caspase-3 activity (Figure 1C). Moreover, the sensitizing effect was dependent on caspase activation as pretreatment of cells with the pan-caspase inhibitor zVADfmk as well as with the specific caspase-9 inhibitor abrogated the effect (Figure 1D and Figure S4). T8 synergistically suppressed the growth of pancreatic carcinoma cells (L3.6pl cells) seeded on the chorioallantoic membrane (CAM) of chicken embryos and treated with etoposide (Figure 1E).

To identify the cellular targets of T8, we applied activity-based protein profiling (ABPP)<sup>[13]</sup> and equipped the molecular scaffold with an alkyne handle as well as a photoreactive group (JP04-042, Figure 2A). Surprisingly, these modifications even increased the chemosensitizing potency of JP04-042 (Figure 2A and Figure S4C).

Next, MDA-MB-231 and HeLa cells were incubated with JP04-042 followed by UV cross-linking to its cellular targets in situ. After cell lysis a rhodamine reporter dye azide was introduced by click chemistry (CC)<sup>[14]</sup> to visualize potential

targets on SDS-PAGE and fluorescent scanning (Figure 2C). Different concentrations of JP04-042 (Figure 2D) and irradiation times (Figure 2E, right panel) were tested. Of note, one dominant protein band appeared at about 63 kDa emphasizing that the probe almost exclusively addressed a single cellular target. To investigate whether the photo probe and the parent T8 molecule bind to the same target, competitive labeling with a constant concentration of JP04-042 versus varying concentrations of competitor T8 was conducted: a 1.5-fold excess of T8 (30  $\mu\text{M}$ ) over JP04-042 (20  $\mu\text{M}$ ) was already sufficient to decrease labeling intensity (Figure 2E, left panel).

Next, the target was identified by a SILAC approach with “heavy” and “medium-weight” isotope-labeled MDA-MB-231 cells. After UV cross-linking and cell lysis either a biotin-PEG-azide or a trifunctional linker (TFL)<sup>[15]</sup> was attached to the probe by CC. Labeled proteins were enriched by a biotin-avidin pull-down. Proteins were either analyzed by SDS-PAGE or prepared for mass spectrometry (MS) by tryptic on-bead digest directly. All independent experiments revealed that PDI and some of its isoforms could be highly enriched

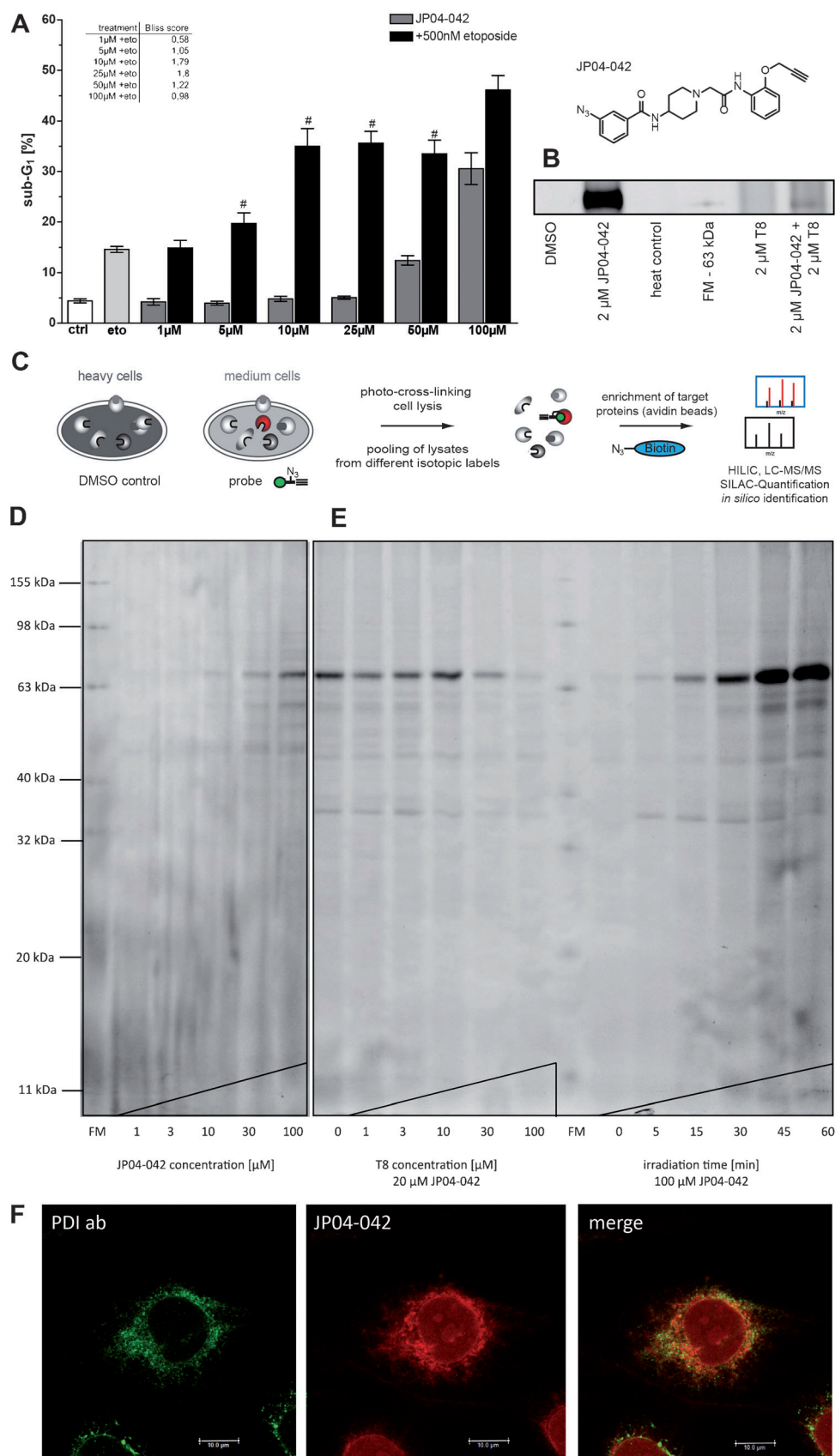


**Figure 2.** Protein labeling, target identification, and validation.

A) Chemical structure of photo probe **JP04-042**. Apoptotic effect of **JP04-042** alone and in combination. # indicates synergy.

B) Labeling of recombinant PDI with **JP04-042** and **T8**. FM: Fluorescent marker. C) Workflow for target identification.

D) Concentration-dependent labeling of MDA-MB-231 cells with **JP04-042**. E) Left: Competitive labeling: 20  $\mu$ M probe, increasing **T8** concentration; right: time-dependent labeling (100  $\mu$ M probe). HeLa cells. F) PDI staining by antibody (green; left) or **JP04-042** (red; middle). Merged picture (right) indicates colocalization of PDI with **JP04-042**.

**Table 1:** Selected hits from quantitative full proteome pull-down and gel-based analysis in isotope-labeled MDA-MB-231 cells.<sup>[a]</sup>

Uniprot ID	Description	gel-based	Fold enrichment probe/DMSO gel-free, replicate			MW [kDa]
			1	2	3	
P07237	protein disulfide isomerase	26	56	41	47	57.1
B3KQT9	cDNA PSEC0175 fis, clone OVARC1000169, highly similar to protein disulfide isomerase A3	18	13	11	27	54.1
P13667	protein disulfide isomerase A4		31	3		72.9

[a] For full lists of proteins see Tables S1–S4 in the Supporting Information.

(see Table 1 and Tables S1–S4 in the Supporting Information).

For target validation, labeling as well as inhibition (see below) of recombinant PDI protein by **JP04-042** was confirmed. Recombinant protein was incubated with the probe and the fluorescent signal vanished when the protein had been pretreated with **T8** or thermally denatured prior to labeling; this suggests that the probe specifically interacts with the folded and active enzyme (Figure 2B).

To verify PDI as a potential target of **JP04-042** in intact cells, **JP04-042**-labeled cells were co-stained with a PDI-specific antibody. MDA-MB-231 cells were incubated with **JP04-042**, irradiated to covalently attach the probe to the target protein, and finally fixed. To visualize the cellular

localization of the probe and PDI, cells were incubated with CC reagents and PDI antibodies, respectively. Hoechst staining was used to mark the nuclei of the cells and background rhodamine binding was determined by the sole addition of CC reagents (Figure S5). Importantly, the PDI-directed antibody as well as the click-dye-conjugated probe overlap in their fluorescent staining, suggesting a consolidated binding to the same target protein (Figure 2F).

In order to explore the structure–activity relationship (SAR) of the **T8**-derived *N*-(1-(2-(R<sup>2</sup>amino)-2-oxoethyl)-piperidin-4-yl)R<sup>1</sup>amide core scaffold, we prepared several new analogues that exhibited diversity in the substituents of the two R<sup>1</sup> and R<sup>2</sup> benzene rings (Figure 3A). Among those, **PS89**, a close analogue of **T8** in which the fluorine in R<sup>1</sup> is

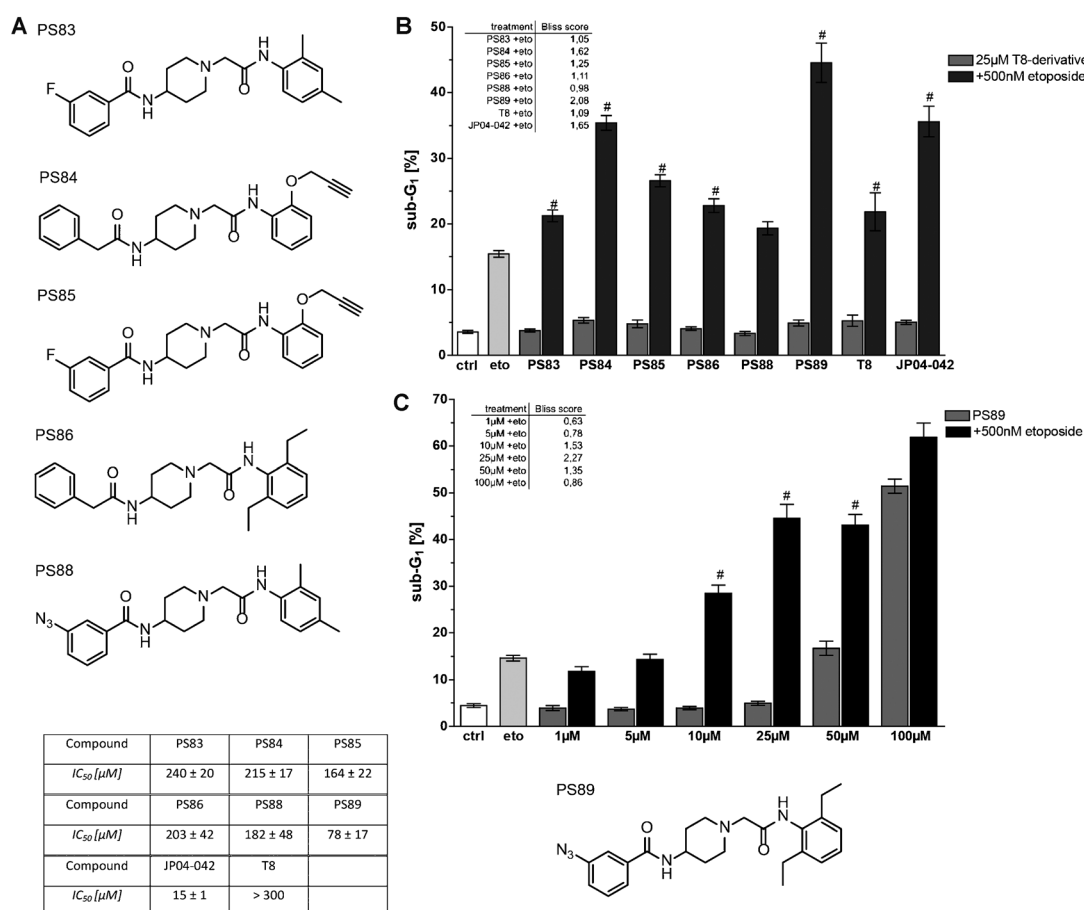


**Figure 3.** **T8** derivatives, inhibition of recombinant PDI, and apoptosis assays. A) Chemical structures of further **T8** derivatives (**PS83–PS89**) and corresponding  $IC_{50}$  values for in vitro PDI inhibition. B) Apoptosis analysis of **T8** derivatives **PS83–PS89** (Jurkat cells) +/– etoposide. C) **PS89** concentration-dependent induction of apoptosis +/– etoposide. # indicates synergy.



replaced by an azide group, displayed the best sensitizing activity of all derivatives in the apoptosis assay with Jurkat cells (Figures 3B and C). Moreover, as described for PDI inhibition the compound is toxic at concentrations above 50  $\mu\text{M}$ . In contrast, **PS88** showed no synergism with etoposide suggesting that a 3,4-dimethyl substitution in the  $\text{R}^2$  ring is less desired. Similar trends could be observed with other cell lines (Figures S4D and E). To show that **PS89** induces ER stress in combination with etoposide, the up-regulation of main proteins involved in ER stress signaling, namely p-eIF2 $\alpha$ , BiP/GRP78, and CHOP, was analyzed by western blot (Figure S6).

To investigate whether the interaction of **T8** and its derivatives with PDI results in the inhibition of enzymatic activity we analyzed all compounds in a turbidimetric insulin assay<sup>[16]</sup> (Table in Figure 3A). **T8** turned out to be only a weak inhibitor in the reductase assay, whereas the probe molecule **JP04-42** and **PS89** revealed concentration-dependent inhibition with  $\text{IC}_{50}$  values down to 15  $\mu\text{M}$ .

An explanation for the differences in the  $\text{IC}_{50}$  values was provided by docking studies with **JP04-42**, **PS89**, and **T8** for the two catalytic sites a and a'. Remarkably, we obtained two preferred binding sites in close proximity ( $\pm 40 \text{ \AA}$ ) to the catalytic centers (Figure S8). A closer inspection of the two sites revealed that they are extended solvent-exposed grooves, which are located on the front and the back side of the catalytic cysteines (Figures 4A and B and Figure S9). However, there are distinct differences in the binding specificities of the **JP04-42** and **PS89** compounds with respect to **T8**. Analysis of the ten energetically best structural clusters (Figure S9) shows that for **JP04-42** and **PS89** several poses shield the catalytic sites, which is a prerequisite of strong inhibition. **T8**, in contrast, binds deeply into the two binding grooves adjacent to each catalytic site (Figure 4C and D). **JP04-42** and **PS89** carry an azide substituent, which perfectly fits into electrostatically complementary deep subpockets within the binding grooves in front of the a and a' sites (Figures 4C and D and Figure S10). In contrast, the diethylphenyl group of **T8** preferentially attaches to predominantly hydrophobic protein interaction sites within the binding groove. Thus, **T8** can be considered an allosteric inhibitor that impairs substrate binding without obstruction of the catalytic cysteines. Of note, although **T8** exhibits a different binding mode it partially overlaps in the pocket with **JP04-42** and **PS89** explaining the observed competition between the inhibitors (Figure 4C). Moreover, this **T8**-specific binding mode may account for the obtained  $\text{IC}_{50}$  differences in the insulin reduction assay (a more detailed discussion is provided in the Supporting Information).

In conclusion, the unique PDI target selectivity, the unprecedented mode of inhibition, and its potent sensitization of cancer cells in various experimental settings place **T8** and optimized derivatives among the most promising com-

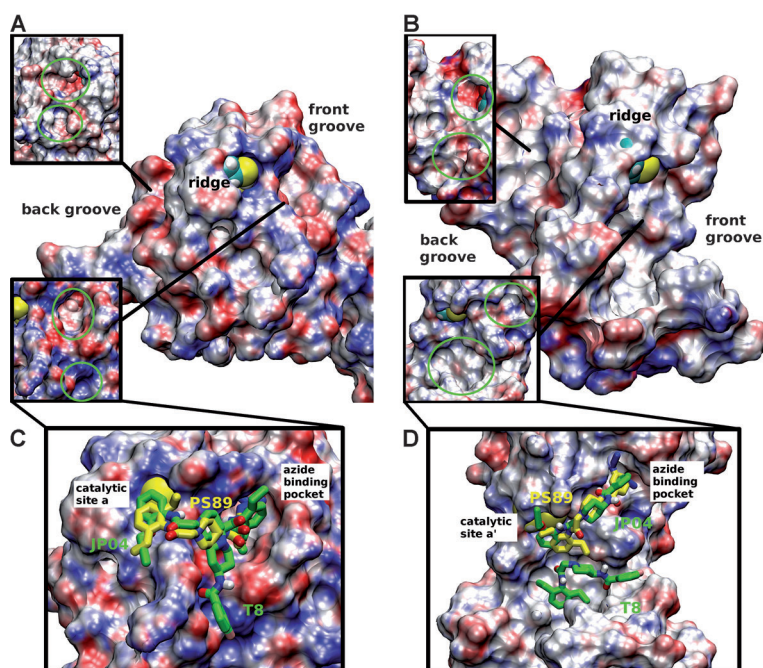


**Figure 4.** Docking experiments. Binding sites at the two catalytic centers in the domains a (A) and a' (B). The two inserted pictures show the back (top insert) and front binding grooves (bottom insert). Deep pockets are indicated by green circles. C,D) Bound structures of **JP04-42** (green), **PS89** (yellow), and **T8** (green) in the two catalytic binding sites, C) domain a, D) domain a'. For the protein its electrostatic potential surface is shown, the ligands are given in green (**JP04-42** and **T8**) and yellow (**PS89**) rod representations colored according to atom type. The graphics were created with VMD.

pounds for further pharmaceutical testing. Most of the previously reported PDI inhibitors are irreversible binders or lack selectivity, both of which are undesired for medicinal applications. The great specificity and reversible mode of action of our **T8** derivatives and their performance in tumor-based assays emphasize a suitable pharmacological profile, which is further substantiated by satisfaction of the Lipinski rules. Furthermore, in-depth analysis of the PDI binding mode and work on apoptotic signaling provides a basis for further exploration of this target in cancer research.

Received: June 30, 2014

Published online: September 26, 2014

**Keywords:** cancer · chemotherapeutics · combination therapy · proteomics · sensitization

- [1] a) C. Holohan, S. Van Schaeybroeck, D. B. Longley, P. G. Johnston, *Nat. Rev. Cancer* **2013**, *13*, 714–726; b) T. R. Wilson, P. G. Johnston, D. B. Longley, *Curr. Cancer Drug Targets* **2009**, *9*, 307–319; c) I. Kim, W. Xu, J. C. Reed, *Nat. Rev. Drug Discovery* **2008**, *7*, 1013–1030.
- [2] B. Luo, A. S. Lee, *Oncogene* **2013**, *32*, 805–818.
- [3] C. Wang, W. Li, J. Ren, J. Fang, H. Ke, W. Gong, W. Feng, C. C. Wang, *Antioxid. Redox Signaling* **2013**, *19*, 36–45.
- [4] a) T. E. Creighton, *BioEssays* **1992**, *14*, 195–199; b) P. T. Varandani, M. A. Nafz, M. L. Chandler, *Biochemistry* **1975**, *14*, 2115–2120; c) N. A. Murkofsky, M. E. Lamm, *J. Biol. Chem.*

- 1979, 254, 12181–12184; d) C. C. Wang, C. L. Tsou, *FASEB J.* **1993**, 7, 1515–1517.
- [5] a) A. M. Benham, *Antioxid. Redox Signaling* **2012**, 16, 781–789; b) S. Xu, S. Sankar, N. Neamati, *Drug Discovery Today* **2014**, 19, 222–240.
- [6] J. Ge, C. J. Zhang, L. Li, L. M. Chong, X. Wu, P. Hao, S. K. Sze, S. Q. Yao, *ACS Chem. Biol.* **2013**, 8, 2577–2585.
- [7] M. M. Khan, S. Simizu, N. S. Lai, M. Kawatani, T. Shimizu, H. Osada, *ACS Chem. Biol.* **2011**, 6, 245–251.
- [8] B. G. Hoffstrom, A. Kaplan, R. Letso, R. S. Schmid, G. J. Turmel, D. C. Lo, B. R. Stockwell, *Nat. Chem. Biol.* **2010**, 6, 900–906.
- [9] R. Banerjee, N. J. Pace, D. R. Brown, E. Weerapana, *J. Am. Chem. Soc.* **2013**, 135, 2497–2500.
- [10] S. Xu, A. N. Butkevich, R. Yamada, Y. Zhou, B. Debnath, R. Duncan, E. Zandi, N. A. Petasis, N. Neamati, *Proc. Natl. Acad. Sci. USA* **2012**, 109, 16348–16353.
- [11] J. C. Tsibris, L. T. Hunt, G. Ballejo, W. C. Barker, L. J. Toney, W. N. Spellacy, *J. Biol. Chem.* **1989**, 264, 13967–13970.
- [12] R. Guthapfel, P. Gueguen, E. Quemeneur, *Eur. J. Biochem.* **1996**, 242, 315–319.
- [13] a) M. J. Evans, A. Saghatelian, E. J. Sorensen, B. F. Cravatt, *Nat. Biotechnol.* **2005**, 23, 1303–1307; b) M. J. Evans, B. F. Cravatt, *Chem. Rev.* **2006**, 106, 3279–3301; c) M. Fonović, M. Bogyo, *Expert Rev. Proteomics* **2008**, 5, 721–730; d) B. F. Cravatt, E. J. Sorensen, *Curr. Opin. Chem. Biol.* **2000**, 4, 663–668; e) P. P. Geurink, L. M. Prely, G. A. van der Marel, R. Bischoff, H. S. Overkleeft, *Top. Curr. Chem.* **2012**, 324, 85–113.
- [14] a) V. V. Rostovtsev, L. G. Green, V. V. Fokin, K. B. Sharpless, *Angew. Chem. Int. Ed.* **2002**, 41, 2596–2599; *Angew. Chem.* **2002**, 114, 2708–2711; b) Q. Wang, T. R. Chan, R. Hilgraf, V. V. Fokin, K. B. Sharpless, M. G. Finn, *J. Am. Chem. Soc.* **2003**, 125, 3192–3193; c) C. W. Tornøe, C. Christensen, M. Meldal, *J. Org. Chem.* **2002**, 67, 3057–3064.
- [15] J. Eirich, J. L. Burkhardt, A. Ullrich, G. C. Rudolf, A. Vollmar, S. Zahler, U. Kazmaier, S. A. Sieber, *Mol. Biosyst.* **2012**, 8, 2067–2075.
- [16] A. M. Smith, J. Chan, D. Oksenberg, R. Urfer, D. S. Wexler, A. Ow, L. Gao, A. McAlorum, S. G. Huang, *J. Biomol. Screening* **2004**, 9, 614–620.